Published in final edited form as:
IEEE Photonics J. 2014 April ; 6(2): . doi:10.1109/JPHOT.2014.2310197.

Breakthrough in Photonics 2013: Photoacoustic Tomography in Biomedicine

Junjie Yao and **Lihong V. Wang***
Optical Imaging Laboratory, Department of Biomedical Engineering, Washington University in St. Louis, One Brookings Drive, St. Louis, Missouri 63130, USA

Abstract

Photoacoustic tomography (PAT) is one of the fastest growing biomedical imaging modalities in the last decade. Building on its high scalability and complementary imaging contrast to other mainstream modalities, PAT has gained substantial momentum in both preclinical and clinical studies. In 2013, PAT has grown markedly in both its technological capabilities and biomedical applications. In particular, breakthroughs have been made in super-resolution imaging, deep blood flow measurement, small animal resting state brain mapping, video rate functional human imaging, and human breast imaging. These breakthroughs have either successfully solved long-standing technical issues in PAT or significantly enhanced its imaging capability. This Review will summarize state-of-the-art developments in PAT and highlight a few representative achievements of the year 2013.

Index terms

Photoacoustic tomography; optical absorption contrast; super-resolution; blood flow; functional human imaging; breast imaging; small animal imaging

1. Introduction

Nowadays, there are many different biomedical imaging modalities. They each have their own different strengths and weaknesses [1]. Generally, the comparative merits of photoacoustic tomography (PAT) over other mainstream modalities can be summarized as follows [2]: (1) compared with optical microscopy, PAT breaks through the optical diffusion limit (~1 mm depth in the skin), with scalable spatial resolution and maximum imaging depth in both the optical and acoustic domains; (2) compared with medical ultrasonography, PAT images optical absorption contrast with 100% relative sensitivity, and provides images without speckle artifacts; (3) compared with fluorescence imaging, PAT can image more molecules, fluorescent or nonfluorescent, at their absorbing wavelengths; (4) compared with X-ray computed tomography (CT), PAT is devoid of ionizing radiation and capable of functional imaging using endogenous contrast agents; and (5) compared with magnetic resonance imaging (MRI) and positron emission tomography (PET), PAT is less expensive

*Corresponding author: lhwang@wustl.edu.

and has better resolution. With these merits, PAT is playing an increasingly important role in biomedical studies, complementing other modalities.

PAT, a relatively young member of the biomedical imaging family, has experienced fast growth in the last two decades, especially since the early 2000s, when its first *in vivo* small animal imaging was demonstrated [3, 4]. In the year 2013, great progress was made in both technical innovations and biomedical applications. This Review will present state-of-the-art PAT technologies, focusing on several breakthroughs in 2013.

2. Highlights in PAT technical innovations

Developments in laser technology, ultrasonic detection, and nanotechnology have driven the advance of PAT. Integrating these developments with novel engineering designs, PAT has been pushing all the limits of its imaging performance over the recent years. Taking advantage of the wide wavelength range of the optical parametric oscillator (OPO), PAT has been used to explore various endogenous imaging contrasts, with primary absorption wavelengths ranging from the ultraviolet to the near-infrared region [5]. Both the lateral and axial resolutions of PAT have approached the theoretical limits in linear imaging. A lateral resolution of 220 nm has been achieved by using a waterimmersion optical objective with a numerical aperture of 1.2 [6]. An axial resolution of ~3 μm has been reported by using a high-frequency ultrasonic transducer with a bandwidth of 400 MHz, although the imaging depth is limited to tens of micrometers [7]. In addition, anatomical features at different geometrical scales can be bettered resolved by using a multi-bandwidth detection method [8]. The imaging depth of PAT has been pushed to ~5 cm in breast phantom [9] and ~7 cm in chicken tissue [2] by using near infrared excitation and low frequency ultrasonic detection. The imaging speed of PAT has been substantially improved to capture dynamic processes. A B-scan frame rate of 20 Hz has been achieved on a photoacoustic (PA) computed tomography system adapted from a commercial ultrasound machine [10]. A B-scan frame rate of 400 Hz has been reported on a water-immersible MEMS scanning mirror based photoacoustic microscope [11]. The detection sensitivity of PAT has been greatly enhanced by using highly absorbing contrast agents, in particular, nanoparticles [12, 13]. PA molecular imaging in deep tissue has been enabled by using reporter gene products [14–16]. In addition to the above achievements, several breakthrough innovations in the year 2013 are highlighted below.

Super-resolution PA imaging was achieved for the first time. Depending on the imaging depth, the spatial resolution of PAT was long limited by acoustic diffraction in the optical diffusive regime or by optical diffraction in the optical ballistic regime. In the optical diffusive regime, Conley et al. and Lai et al. reported a sub-acoustic-diffraction imaging method by using the photoacoustic signal as feedback for the wavefront shaping optimization [17, 18]. Conley et al.'s method takes advantage of the non-uniform detection sensitivity of a focused ultrasonic transducer. Photoacoustic imaging behind a scattering medium was demonstrated with a resolution of ~13 μm, five to six times smaller than the acoustic diffraction limit [17]. Based on the Grueneisen memory effect, Lai et al.'s method utilizes the nonlinear PA signals as feedback to guide iterative wavefront optimization [18]. Here, the Grueneisen memory effect describes the fact that, within the thermal confinement

time, the temperature rise due to the absorption of light lingers and changes the local Grueneisen parameter accordingly. Experimental results demonstrated an optical diffraction-limited focus on the scale of 5–7 μm in scattering media, ten times smaller than the acoustic diffraction limit, with an enhancement factor of ~6,000 in peak fluence [18]. In optical ballistic regime, Yao et al. overcame the optical-diffraction limit by using the excitation-intensity dependence of the photobleaching effect (Figure 1a) [19]. They have demonstrated PA imaging of gold nanoparticles with a resolution of ~80 nm, three times smaller than the optical diffraction limit (Figure 1b). Another sub-optical-diffraction PA imaging method was reported by Nedosekin et al. with a resolution of ~100 nm for nanoparticles, where nonlinear signal amplification by nanobubbles circumvented the optical diffraction limit [20]. These works have demonstrated PAT as the only imaging modality that can break both the optical diffusion limit and optical diffraction limit.

Deep tissue blood flow measurement by PAT was achieved for the first time. To apply existing PA blood flow measurement methods in deep tissue, a long-standing hurdle was their requirement of resolvable absorbers in the flowing medium, which was particularly challenging when only acoustic-resolution was available. Wang et al. successfully resolved this issue by thermally tagging a small portion of the flowing blood and photoacoustically monitoring the tagged ‘hot’ blood (Figures 2a–b) [21, 22]. Because the tagged blood serves as an acoustically defined ‘virtual absorber’, blood flow can be measured deep in tissue. This new method has been implemented in both acousticresolution photoacoustic microcopy and photoacoustic computed tomography. A flow measurement sensitivity of 0.25 mm/s has been achieved at 5 mm depth in tissue (Figure 2c). In addition to blood flow dynamics, this work also opens the window for deep-tissue metabolic studies that require blood flow information.

3. Highlights in PAT biomedical applications

Translating cutting-edge PAT technologies to small animal and human imaging is the key to realizing the impact. So far, PAT has been explored in numerous preclinical and clinical studies. In particular, PAT has made considerable progress in detecting early-stage cancers [23], assessing skin lesions [24], imaging brain activities [25], mapping sentinel lymph nodes [26], monitoring drug or contrast agent delivery [27, 28], and performing endoscopic examinations [29]. The following achievements in the year 2013 particularly deserve to be highlighted.

First, noninvasive functional imaging of small-animal brain has been demonstrated with high spatial-temporal resolution. Mapping brain structure and function is one of the most exciting fields of science. However, functional magnetic resonance imaging (fMRI), the most commonly used functional brain imaging tool, lacks the spatial-temporal resolution for fast small animal brain imaging. Using the full-ring-array PA computed tomography system, Nasiriavanaki et al. successfully achieved functional connectivity imaging of the mouse brain at resting state, with an in-plane resolution of 100 μm and a frame rate of 0.6 Hz [25]. The results, shown in Figure 3, clearly indicate bilateral correlations in eight main functional regions, as well as in several subregions. A unique advantage of PAT is that the functional

connectivity maps are automatically co-registered with high-resolution cortical vascular images, allowing pinpoint location of neural activities.

Second, noninvasive label-free three-dimensional PA imaging of human tissues/organs has been demonstrated with substantially improved imaging quality. Human imaging is no doubt the most important area in PAT development. However, PAT systems adapted from commercial ultrasound machines with linear arrays are usually limited to 2D imaging [10, 30]. Recently, Dean-ben et al. have improved functional PA human imaging to a volumetric frame rate of 10 Hz [31]. In this important work, a spherically arranged 256-element 2D ultrasonic array and near-infrared excitations in the region between 700 and 860 nm are combined to provide *in vivo* imaging of human tissue vasculature, blood oxygenation and hemodynamic changes, as shown in Figures 4a–d. However, 256 elements are considered too sparse for a 2D array, tending to cause imaging artifacts outside the central zone of the 3D field of view covered by the array. A denser 2500- element 2D planar array was explored previously by Wang et al. [32]; however, the data acquisition required multiplexing. Kruger et al. have developed a dedicated 3D PA mammography system capable of imaging blood vessels in human breasts with submillimeter spatial resolution (Figures 4e–f) [9]. Compared with previously reported PA mammography systems, this work shows significantly improved field of view, contrast to noise ratio and spatial resolution. All of these advances are important maturing steps of PAT towards human imaging. However, the depths of the blood vessels from the nearest skin surface are unclear from the images.

4. Conclusions

2013 was a productive year for the entire PA community, and we can cover only a small portion of the achievements in this Review. The studies reported here demonstrate the strong multiparametric imaging capability of PAT for small animals and humans, and more importantly, the momentum of the fast growth of PAT in biomedicine. With a series of long-standing engineering challenges overcome, we believe that PAT will see even faster growth in the coming years. In particular, translational PAT will still be the most exciting area that expects breakthroughs, especially in early cancer detection [33], human breast imaging [34] and endoscopic imaging [29]. Functional human brain imaging by PAT will gain more attentions, and it is just a matter of time before PAT becomes an important tool for neuroscience studies, complementing other brain imaging modalities. Another promising area is reporter-gene–based molecular PA imaging, where genetically encoded PA contrast allows selective labelling of cells and permits studies of specific biological behaviors *in vivo* [16].

Acknowledgments

The authors appreciate Prof. James Ballard’s close reading of the manuscript. This work was sponsored by NIH grants DP1 EB016986 (NIH Director’s Pioneer Award), R01 CA186567 (NIH Director’s Transformative Research Award), R01 EB016963, R01 CA134539, R01 EB010049, R01 CA157277, and R01 CA159959. L. V. Wang has a financial interest in Endra, Inc., and Microphotoacoustics, Inc., which, however, did not support this work.

References

1. Wang, LV.; Wu, H-i. Biomedical optics : principles and imaging. Hoboken, N.J.: Wiley-Interscience; 2007. p. xivp. 362
2. Wang LHV, Hu S. Photoacoustic Tomography: In Vivo Imaging from Organelles to Organs. Science. 2012; 335(6075):1458–1462. [PubMed: 22442475]
3. Zhang HF, Maslov K, Stoica G, Wang LHV. Functional photoacoustic microscopy for high-resolution and noninvasive in vivo imaging. Nature Biotechnology. 2006; 24(7):848–851.
4. Wang XD, Pang YJ, Ku G, Xie XY, Stoica G, Wang LHV. Noninvasive laser-induced photoacoustic tomography for structural and functional in vivo imaging of the brain. Nature Biotechnology. 2003; 21(7):803–806.
5. Beard P. Biomedical photoacoustic imaging. Interface Focus. 2011; 1(4):602–631. [PubMed: 22866233]
6. Zhang C, Maslov K, Wang LHV. Subwavelength-resolution label-free photoacoustic microscopy of optical absorption in vivo. Optics Letters. 2010; 35(19):3195–3197. [PubMed: 20890331]
7. Strohm EM, Berndl ESL, Kolios MC. Probing Red Blood Cell Morphology Using High-Frequency Photoacoustics. Biophysical Journal. 2013; 105(1):59–67. [PubMed: 23823224]
8. Gateau J, Chekkoury A, Ntziachristos V. Ultra-wideband three-dimensional optoacoustic tomography. Opt Lett. 2013; 38(22):4671–4674. [PubMed: 24322102]
9. Kruger RA, Kuzmiak CM, Lam RB, Reinecke DR, Del Rio SP, Steed D. Dedicated 3D photoacoustic breast imaging. Medical physics. 2013; 40(11):113301. [PubMed: 24320471]
10. Montilla LG, Olafsson R, Bauer DR, Witte RS. Real-time photoacoustic and ultrasound imaging: a simple solution for clinical ultrasound systems with linear arrays. Physics in medicine and biology. 2013; 58(1):N1–N12. [PubMed: 23221479]
11. Yao JJ, Huang CH, Wang LD, Yang JM, Gao L, Maslov KI, Zou J, Wang LHV. Wide-field fast-scanning photoacoustic microscopy based on a water-immersible MEMS scanning mirror. Journal of Biomedical Optics. 2012; 17(8):080505. [PubMed: 23224156]
12. De La Zerda A, Zavaleta C, Keren S, Vaithilingam S, Bodapati S, Liu Z, Levi J, Smith BR, Ma TJ, Oralkan O, Cheng Z, Chen XY, Dai HJ, Khuri-Yakub BT, Gambhir SS. Carbon nanotubes as photoacoustic molecular imaging agents in living mice. Nature Nanotechnology. 2008; 3(9):557–562.
13. Zackrisson S, van de Ven SM, Gambhir SS. Light in and sound out: emerging translational strategies for photoacoustic imaging. Cancer Res. 2014; 74(4):979–1004. [PubMed: 24514041]
14. Razansky D, Distel M, Vinegoni C, Ma R, Perrimon N, Koster RW, Ntziachristos V. Multispectral opto-acoustic tomography of deep-seated fluorescent proteins in vivo. Nature Photonics. 2009; 3(7):412–417.
15. Cai X, Li L, Krumholz A, Guo ZJ, Erpelding TN, Zhang C, Zhang Y, Xi YN, Wang LHV. Multi-Scale Molecular Photoacoustic Tomography of Gene Expression. Plos One. 2012; 7(8):e43999. [PubMed: 22952846]
16. Laufer J, Jathoul A, Pule M, Beard P. In vitro characterization of genetically expressed absorbing proteins using photoacoustic spectroscopy. Biomedical Optics Express. 2013; 4(11):2477–2490. [PubMed: 24298408]
17. Conkey, Donald B.; Caravaca-Aguirre, Antonio M.; Dove, Jacob D.; Ju, Hengyi; Murray, Todd W.; Piestun, R. Super-resolution photoacoustic imaging through a scattering wall. arXiv. 2013 **1310.5736**.
18. Lai P, Wang L, Tay JW, Wang L. Nonlinear photoacoustic wavefront shaping (PAWS) for single speckle-grain optical focusing in scattering media. arXiv. 2014 **arXiv:1402.0816**.
19. Yao J, Wang L, Li C, Zhang C, Wang LV. Photoimprint Photoacoustic Microscopy for Three-Dimensional Label-Free Subdiffraction Imaging. Physical Review Letters. 2014; 112(1):014302. [PubMed: 24483902]
20. Nedosekin DA, Galanzha EI, Dervishi E, Biris AS, Zharov VP. Super-resolution nonlinear photothermal microscopy. Small. 2014; 10(1):135–142. [PubMed: 23864531]

21. Wang L, Yao J, Maslov KI, Xing W, Wang LV. Ultrasound-heated photoacoustic flowmetry. Journal of Biomedical Optics. 2013; 18(11):117003. [PubMed: 24194064]
22. Wang LD, Xia J, Yao JJ, Maslov KI, Wang LHV. Ultrasonically Encoded Photoacoustic Flowgraphy in Biological Tissue. Physical Review Letters. 2013; 111(20):204301. [PubMed: 24289689]
23. Wilson KE, Wang TY, Willmann JK. Acoustic and Photoacoustic Molecular Imaging of Cancer. Journal of Nuclear Medicine. 2013; 54(11):1851–1854. [PubMed: 24187042]
24. Vionnet L, Gateau J, Schwarz M, Buehler A, Ermolayev V, Ntziachristos V. 24-MHz Scanner for Optoacoustic Imaging of Skin and Burn. Medical Imaging, IEEE Transactions on. 2014; 33(2): 535–545.
25. Nasiriavanaki M, Xia J, Wan H, Bauer AQ, Culver JP, Wang LV. High-resolution photoacoustic tomography of resting-state functional connectivity in the mouse brain. Proc Natl Acad Sci U S A. 2014; 111(1):21–26. [PubMed: 24367107]
26. Bayer CL, Joshi PP, Emelianov SY. Photoacoustic imaging: a potential tool to detect early indicators of metastasis. Expert Rev Med Devices. 2013; 10(1):125–134. [PubMed: 23278229]
27. Gong H, Peng R, Liu Z. Carbon nanotubes for biomedical imaging: The recent advances. Adv Drug Deliv Rev. 2013; 65(15):1951–1963. [PubMed: 24184130]
28. Tsyboulski DA, Liopo AV, Su R, Ermilov SA, Bachilo SM, Weisman RB, Oraevsky AA. Enabling in vivo measurements of nanoparticle concentrations with three-dimensional optoacoustic tomography. Journal of biophotonics. 2013 **Early publication**.
29. Yang JM, Favazza C, Chen RM, Yao JJ, Cai X, Maslov K, Zhou QF, Shung KK, Wang LHV. Simultaneous functional photoacoustic and ultrasonic endoscopy of internal organs in vivo. Nature Medicine. 2012; 18(8):1297–1302.
30. Erpelding TN, Kim C, Pramanik M, Jankovic L, Maslov K, Guo ZJ, Margenthaler JA, Pashley MD, Wang LHV. Sentinel Lymph Nodes in the Rat: Noninvasive Photoacoustic and US Imaging with a Clinical US System. Radiology. 2010; 256(1):102–110. [PubMed: 20574088]
31. Dean-Ben XL, Razansky D. Functional optoacoustic human angiography with handheld video rate three dimensional scanner. Photoacoustics. 2013; 1(3–4):68–73. [PubMed: 25302151]
32. Wang Y, Erpelding TN, Jankovic L, Guo ZJ, Robert JL, David G, Wang LHV. In vivo three-dimensional photoacoustic imaging based on a clinical matrix array ultrasound probe. Journal of Biomedical Optics. 2012; 17(6):061208. [PubMed: 22734738]
33. Stritzker J, Kirscher L, Scadeng M, Deliolanis NC, Morscher S, Symvoulidis P, Schaefer K, Zhang Q, Buckel L, Hess M, Donat U, Bradley WG, Ntziachristos V, Szalay AA. Vaccinia virus-mediated melanin production allows MR and optoacoustic deep tissue imaging and laser-induced thermotherapy of cancer. Proceedings of the National Academy of Sciences of the United States of America. 2013; 110(9):3316–3320. [PubMed: 23401518]
34. Heijblom M, Piras D, Maartens E, Huisman EJ, van den Engh FM, Klaase JM, Steenbergen W, Manohar S. Appearance of breast cysts in planar geometry photoacoustic mammography using 1064-nm excitation. Journal of Biomedical Optics. 2013; 18(12):126009. [PubMed: 24343440]

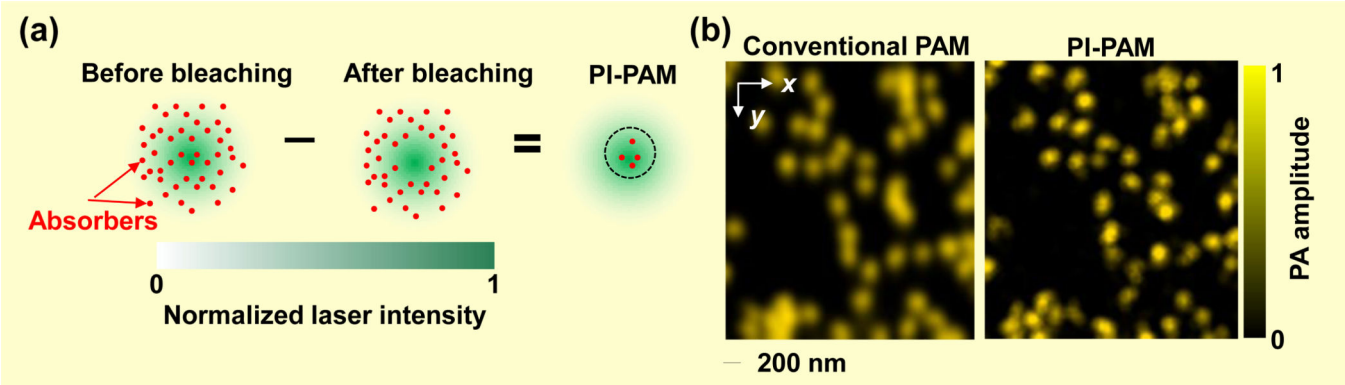

Figure 1. Advance in PA super-resolution imaging

(a) Photo-imprint PA microscopy (PI-PAM) based on the photobleaching rate dependence on the local excitation intensity. The first excitation bleaches the center part of the illuminated region more than the periphery, leaving an imprint in the sample. The differential signal between the before- (left panel) and after-bleaching (middle panel) images results in a smaller effective excitation size and thus a resolution enhancement, as shown by the dashed circle in the right panel. (b) PI-PAM imaging of gold nanoparticles with enhanced lateral resolution of ~80 nm. Adapted with permission from [19].

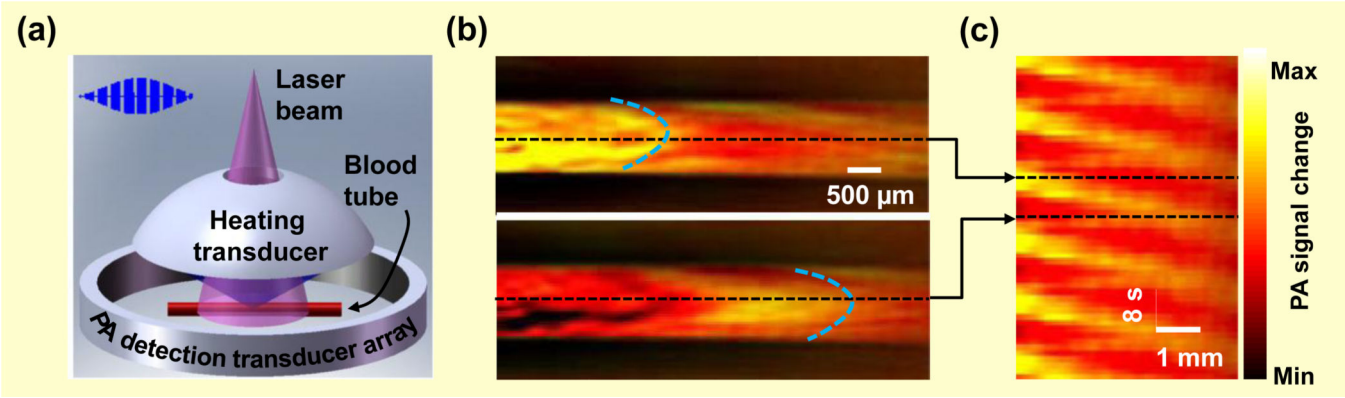

Figure 2. Advance in PA deep tissue blood flow measurement

(a) Schematic of ultrasonically encoded photoacoustic flowgraphy, where part of the flowing blood is thermally tagged by a heating transducer. The movement of the tagged blood is imaged by a circular-array-based PA computed tomography system. (b) Snapshot PA images of the thermally tagged blood flowing in a plastic tube covered by 5-mm-thick chicken breast tissue. The two images are 9 seconds apart, and the flow is from left to right. The curved dashed line shows a parabolic heating peak propagating with blood flow. (c) Flow trajectories in the time-space plane, showing an *en face* spatial-temporal assembling of the measured temperature distribution of the flowing medium. Each horizontal line in the figure is extracted from one photoacoustic image along the flow direction, as shown by the black dashed line in (b). The flow speed and direction can be extracted from the slope of the trajectory. Adapted with permission from [22].

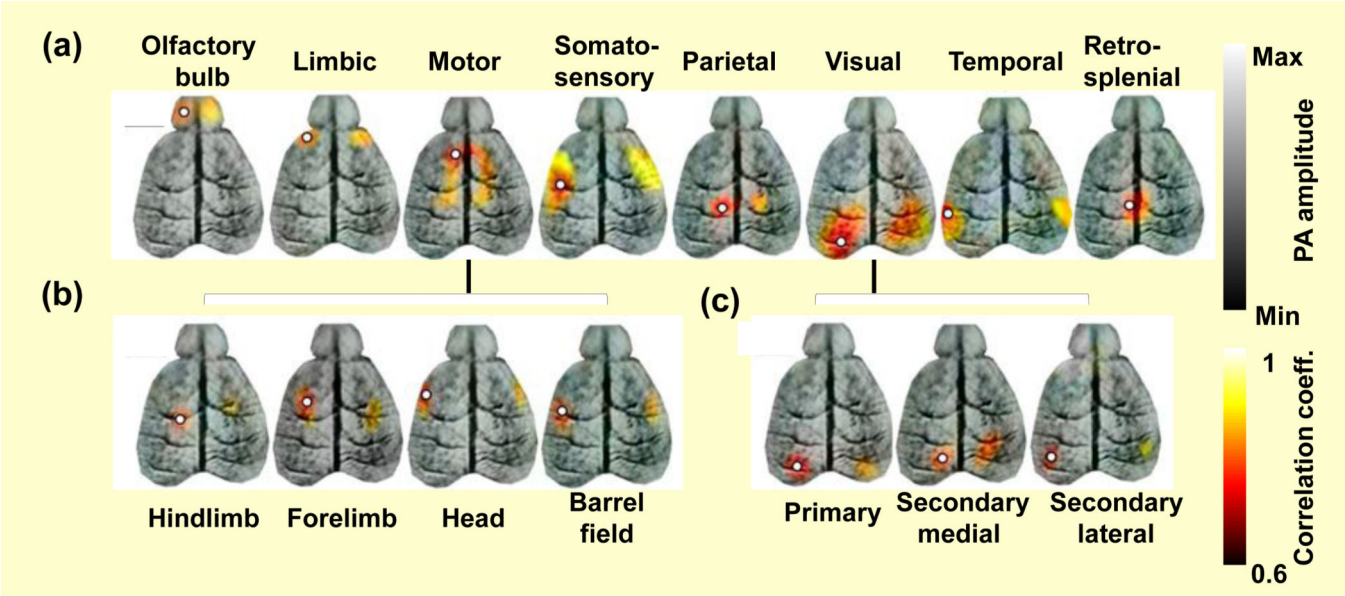

Figure 3. Functional connectivity maps in a live mouse brain acquired noninvasively by PAT

Correlation maps of (a) the eight main functional regions, (b) the four subregions of the somatosensory cortex, and (c) the three subregions of the visual cortex. Adapted with permission from [25].

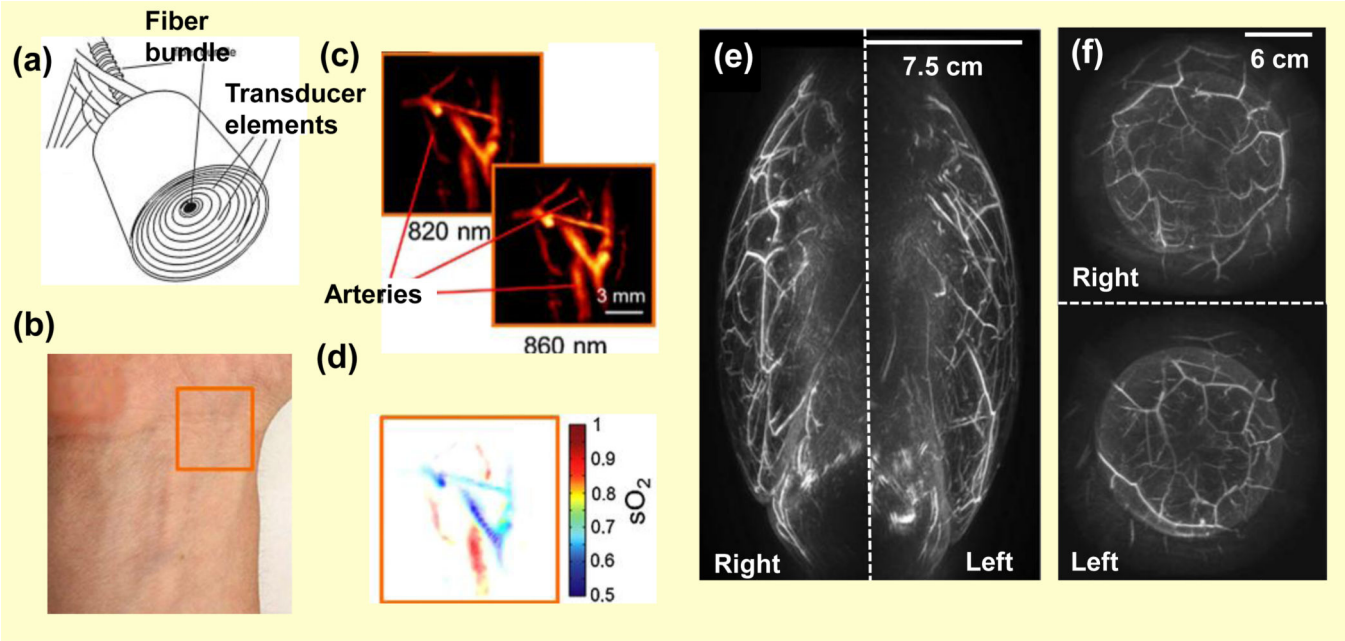

Figure 4. Advances in PA human imaging in the year 2013

(a) Schematic of the clinical hand-held PAT probe for high resolution 3D human imaging at video rate. (b) Photograph of a volunteer's wrist region imaged by the hand-held PAT probe. (c) Maximum amplitude projection images acquired at two different wavelengths in the near-infrared region. Arteries and veins can be readily identified by their spectral information. (d) PAT of the oxygen saturation of hemoglobin (sO_2), as calculated from images acquired at different wavelengths in (c). (e) Medial-lateral maximum amplitude projection of bilateral PAT breast images of a healthy volunteer. (f) Coronal maximum amplitude projection of bilateral PAT breast images of the same volunteer. Adapted with permission from [9, 31].